*Article citation info:*
Grochowalska J, Wrzask K, Kapusta Ł. Proper orthogonal decomposition analysis of an atomized fuel spray of marine diesel engine. Combustion Engines. 2026;204(1):167-175. https://doi.org/10.19206/CE-210467

*Joanna GROCHOWALSKA*
*Klaudia WRZASK*
*Łukasz KAPUSTA*

**Combustion Engines**
**Polish Scientific Society of Combustion Engines**

# Proper orthogonal decomposition analysis of an atomized fuel spray of marine diesel engine

ARTICLE INFO

Received: 13 June 2025
Revised: 4 September 2025
Accepted: 8 September 2025
Available online: 26 September 2025

*Most marine vessels are powered by diesel engines. Unfortunately, fuel combustion releases harmful toxic compounds into the atmosphere. The International Maritime Organization (IMO) regulates these emissions, making their reduction essential for engineers and scientists. The fuel combustion process in a marine diesel engine's cylinder precedes the fuel spray injection and atomization. Fuel spray's flow fluctuations and vortex structures significantly impact the combustion. This paper presents research using the Mie Scattering optical technique to analyze snapshot sequences of spray patterns recorded with a high-speed camera. These snapshots are the results of experimental research on atomized fuel sprays with a marine diesel engine injector within a constant volume chamber. The influence of different chamber backpressures on the fuel spray is studied. The Proper Orthogonal Decomposition (POD) method is promising for quantitatively analyzing spray structures and flow characteristics. This research demonstrates how different chamber conditions affect the decay of the POD singular values, which typically indicate flow characteristics like coherence and fluctuations.*

Key words: *marine diesel engine, fuel sprays, Mie scattering optical technique, POD method, fuel flow characteristics*



## 1. Introduction

Maritime shipping is one of the most important transport sectors utilized in international trade for the transportation of goods, with most sea vessels traveling between continents. Marine vessels primarily use diesel engines for main and auxiliary propulsion. These marine diesel engines commonly burn heavy fuel oil (HFO) and marine diesel oil (MDO). Combustion of these fuels produces exhaust gases containing nitrogen oxides ($NO_x$), sulfur oxides ($SO_x$), carbon monoxide (CO), and particulate matter, significantly contributing to air pollution in marine environments [8, 19]. According to the International Maritime Organization (IMO), shipping emissions accounted for around 3% of global emissions in 2018 [9]. Despite ongoing development and introduction of alternative propulsion technologies and fuels, diesel engines continue to be the predominant equipment in vessel power plants. Diesel engines dominate maritime transport due to their reliability and established infrastructure, indicating that the shift to alternatives will be gradual. It becomes reasonable for engineers and scientists to work on improving the quality of fuel combustion in marine diesel engines. According to Deng [3], emission reduction strategies for diesel engines can be categorized into fuel optimization, pre-combustion control technologies, and exhaust after-treatment systems. The combustion process in marine diesel engine cylinders is characterized by dynamic, interdependent phenomena, with fuel atomization quality playing a critical role. Factors influencing fuel atomization include fuel injection pressure [4, 10, 17], fuel properties [16], and fuel injector nozzle geometry [22]. Furthermore, in [21], the authors show that the exhaust gas composition strongly depends on the opening pressure of the fuel injector.

When fuel is injected into the combustion chamber under high injection pressure, it is atomized, rapidly evaporates, and mixes with compressed air. The first stage of fuel jet breakup is called the primary breakup. This stage of fuel spray breakup is very important, as it determines the initial size and distribution of the resulting droplets, which directly affect the efficiency of atomization and subsequent atomization processes.

In the second stage, the disintegration of the fuel jet occurs under the influence of aerodynamic forces from the surrounding medium. Droplets formed by separation from the liquid core subsequently undergo secondary disintegration. In this context, assessing the quality of fuel atomization in internal combustion engines with direct cylinder fuel injection is crucial to achieving optimal combustion, energy efficiency, and low exhaust emissions [15]. Atomization quality is assessed based on the spray pattern and droplet distribution. It is not possible to directly measure the fuel atomization process inside the cylinder during engine operation. Therefore, specialized experimental setups equipped with constant volume chambers are typically used to investigate the fuel atomization process [6, 7, 23]. Fuel injection and atomization are rapidly changing phenomena. Optical imaging provides dynamic insights into the structural evolution of fuel sprays over time, necessitating sophisticated image processing techniques that accurately preserve structural characteristics [18]. It should also be noted that measuring droplet diameters in diesel sprays poses a challenge due to the small droplet size and high optical density, which significantly limit the range of techniques available for characterizing spray microstructure [13].

In this study, we explore the application of Proper Orthogonal Decomposition (POD) as an effective method for analyzing and quantifying the fuel atomization processes.

The POD method has been applied across various fields, including signal analysis, data compression, and image processing. In the context of fluid mechanics, POD was first introduced by Lumley [14] and was primarily used to describe turbulent flows quantitatively [1]. POD also finds application in Computational Fluid Dynamics (CFD), particularly for dimensionality reduction [5]. This technique has become a popular and effective analysis tool in engine research. It has been successfully used to identify turbulent flows and fluctuations generated by the intake port of a direct injection spark ignition engine [11]. In [2], the authors demonstrated that POD can be applied to identify and quantify cyclic variations in intake air motion and spray structure under running engine conditions. Additionally, Weiss [20] offers a practical and intuitive tutorial on the POD method for fluid mechanics engineers, including MATLAB code examples.

This paper aims to present the application of the POD method for the preliminary analysis of the fuel injection processes inside the cylinder of a marine diesel engine. To this end, experimental results of fuel spray characteristics obtained in a constant volume chamber using a marine diesel engine injector were utilized. Integrating POD with high-speed imaging allows for decomposing complex spray behavior into low-order coherent modes and higher-order dynamics, which represent time–varying fuel flow structures and spray characteristics. In this work, the POD method was used for the preliminary assessment of the effect of changes in backpressure in a constant volume chamber on the characteristics of the fuel spray, in particular, turbulent flows and fluctuations. Through this approach, we aim to contribute to a better understanding of the fuel-air mixing and atomization process in application to design more efficient and cleaner marine combustion systems.

## 2. Experimental setup

This article presents laboratory research [6, 7]. The selected parameters are consistent with those typically observed in marine diesel engines. The fuel injector used in this research is part of the Sulzer Al 25/30 marine diesel engine injection system. The fuel injector system operated on the basis of a common-rail configuration. Therefore, the high-pressure fuel system (UPS – Unit Pump System) maintained a constant pressure of approximately 50 MPa. Only one hole diameter of the fuel injector was active, and the others were plugged. The nozzle diameter was 0.285 mm, and the L/D coefficient was practically 10.9, where L is the hole length and D is the hole diameter. The presented experimental tests were carried out at ambient temperature, and the fuel injection time was 0.04 s. Diesel fuel with a density of 816.1 kg/m³ at 40°C was used in this research. One of the main elements of the experimental setup was the constant volume chamber, presented in Fig. 1.

The constant volume chamber was equipped with access windows measuring 100 mm in diameter and was filled with inert gas nitrogen. Backpressures of 3.2 MPa and 4.3 MPa in the constant volume chamber were considered. These backpressures correspond to the cylinder pressures in the marine diesel engine Sulzer 3 Al 25/30 at the start of injection, 18° before top dead center, operating under low and high load conditions. The conditions of experimental research were presented in Table 1.

The mechanical injector was calibrated to fuel opening pressures of 15 MPa and 25 MPa, respectively, using a spring needle adjustment. The fuel pressure before the injector was measured with a piezoresistive pressure sensor, Kistler type 4067E [12]. The process of fuel injection into the constant volume chamber was visualized using the optical Mie scattering method with a high-speed Photron SA 1.1 camera, operating at a recording frequency of 15 kHz. The laboratory experimental setup is presented in Fig. 2. The Mie scattering optical technique requires appropriate lighting. Therefore, two halogen lamps of 500 W each were used to illuminate the fuel injection into the constant volume chamber.

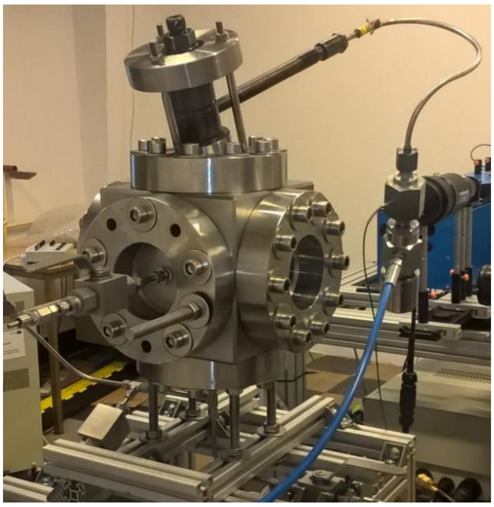

Fig. 1. The constant volume chamber

Table 1. Conditions of experimental research

| Parameter | Value | Unit |
|---|---|---|
| Injector opening pressure | 15, 25 | MPa |
| Backpressure | 3.2, 4.3 | MPa |
| Injector opening time | 0.04 | s |
| Nozzle diameter | 0.285 | mm |
| L/D | 10.9 | – |
| Shape of the hole | cylindrical | – |
| Test temperature | 293–298 | K |
| Diesel oil properties | | |
| Density (at 40°C) | 816.1 | kg/m$^3$ |
| Viscosity | 2.35 | mPa·s |

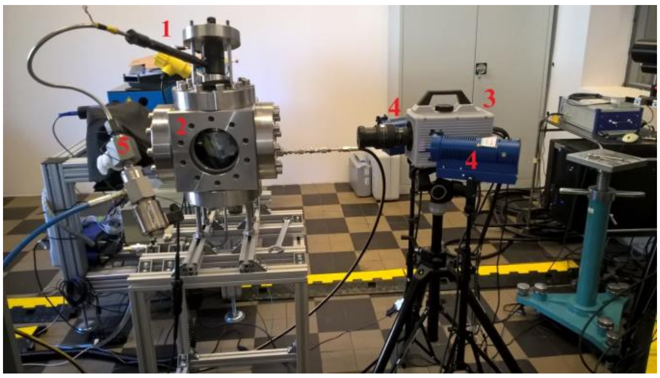


Fig. 2. The experimental set-up: 1 – marine diesel engine fuel injector, 2 – constant volume chamber, 3 – high–speed camera Photron 1.1, 4 – halogen lamps, 5 – fuel pressure sensor [6]

To assess the repeatability of the experiment, tests were conducted three times under each chamber condition. Further in the text, these tests are referred to as runs 1–3. The process of fuel injection into a constant volume chamber was recorded from the beginning to the complete development of the spray. As a result, a series of photographs was obtained for each measurement, of which 180 images were selected for analysis. Fig. 3 presents example spray images.

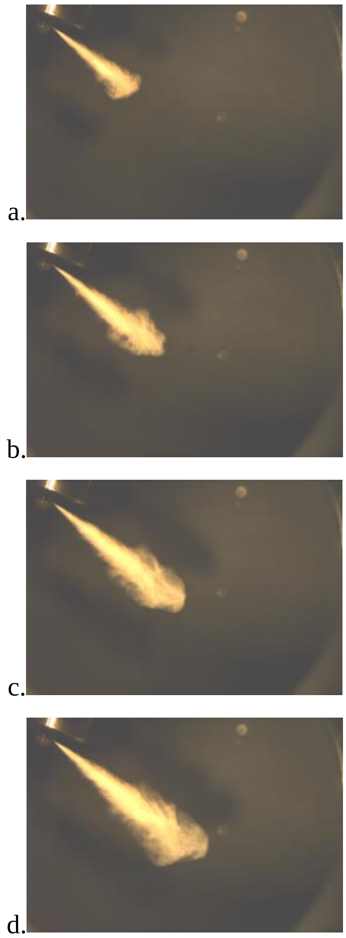


Fig. 3. Example images of fuel spray at an injector opening pressure of 25 MPa and a backpressure 3.2 MPa; time after start of fuel injection: a. 0.9 ms, b. 1.4 ms, c.1.9 ms, d. 2.4 ms

## 3. Data processing

To analyze the dynamic characteristics of the fuel spray, we used the POD method. POD is a technique to extract the dominant patterns from dynamically changing data, such as a sequence of spray images. It decomposes the data into spatial modes and associated time coefficients, ordered according to the most energetic structures. In this section, we explain all the steps needed to perform POD.

- Step 1: Preprocessing

For preprocessing, we first converted all images to grayscale. Then, we normalized the data within each test to eliminate differences in exposure and illumination between snapshots. Next, we ensured that the spray appeared in the same location across all snapshots and that the injection start time was consistent for all cases. This resulted in 180 snapshots per fuel spray test. Given the camera sampling rate of 15 kHz, this corresponded to 12 ms of analyzed time. The analyzed image dimensions of 464 × 710 pixels.

- Step 2: Data centering

In this step, we first calculate the mean field by averaging all the snapshots across the same test. Next, the mean field was subtracted from each snapshot, resulting in a centered dataset.

$$X' = X - \overline{X} \quad (1)$$

By performing this step, we ensure that POD will capture only the meaningful dynamics structure of the fuel spray. Further, in the POD decomposition, the average spray pattern $\overline{X}$ represents the steady-state structure and will be referred to as the zero-th mode.

- Step 3: Data organization

Additionally, we conducted image vectorization, where each 2D snapshot was transformed into a 1D vector. These vectors were then organized as columns in a data matrix $X' \in R^{m \times n}$, where m represents the number of pixels per image and n denotes the number of snapshots. In this case, it was m = 329440 and n = 180.

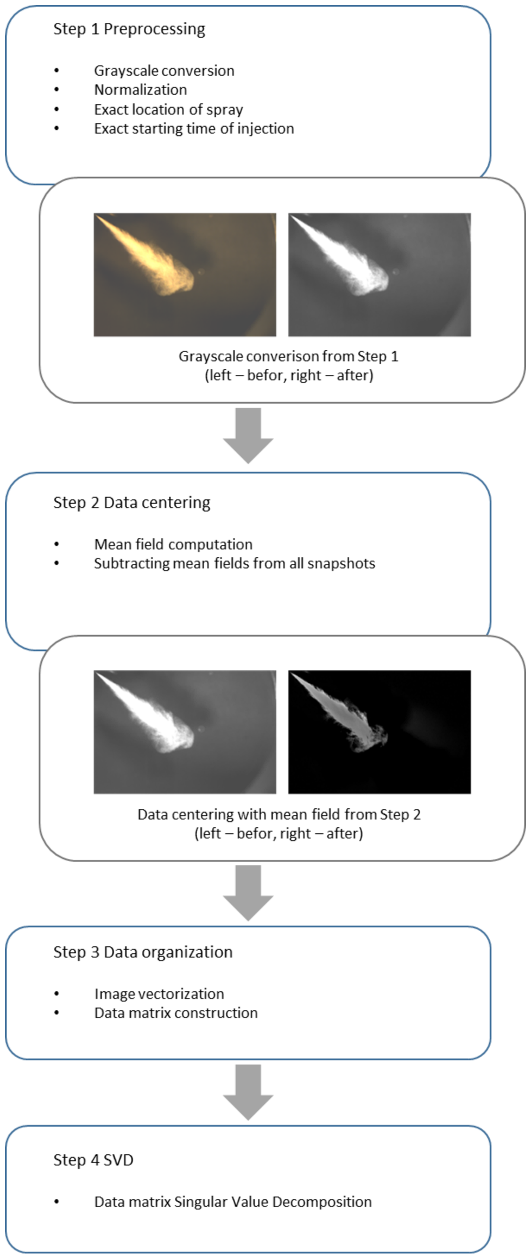


Fig. 4. Flowchart of the main steps to perform POD on a sequence of image data

- Step 4: Singular Value Decomposition (SVD)

The centered data matrix $X'$ undergoes the Singular Value Decomposition (SVD):

$$X' = U\Sigma V^T \quad (2)$$

As a result of such data decomposition, we obtain $U \in R^{m\times n}$ – a matrix that contains the spatial modes, $\Sigma \in R^{n\times n}$ – a diagonal matrix with singular values $\sigma_i$ representing each mode's energy, and $V \in R^{n\times n}$ – contains temporal coefficients showing how each mode evolves in time.

As a summary, in Fig. 4 we present a flowchart of all the steps needed to perform POD on a sequence of image data.

## 4. Result analysis

### 4.1. Singular value analysis

In this section, we present an analysis based on the POD decomposition of a sequence of snapshots – including the singular values, spatial modes, and temporal coefficients – and explain the physical interpretation of the results.

A flowchart of the possible POD analysis for spray injection dynamics, taking into account the singular values, spatial modes, and temporal coefficients, is presented in Fig. 5.

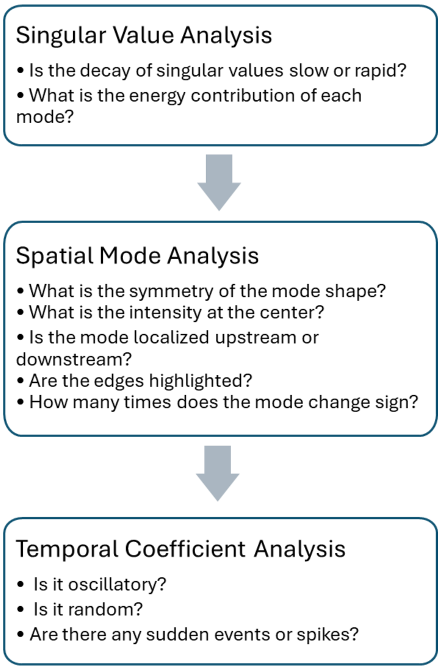


Fig. 5. Flowchart of the POD analysis

As a result of the POD decomposition on spray snapshots, we first present the singular values $\sigma_i$ from the $\Sigma$ matrices for each test run. The experimental trials that were conducted under the same pressure conditions are marked with the same color. In Fig. 6, the first ten singular values are presented for all experimental trials.

A rapid decay in singular values suggests that the system is dominated by a few coherent modes, which is typical in structured fluid flows. In contrast, a slow decay indicates the presence of many contributing modes and points to more complex or potentially turbulent dynamics. Further, in Fig. 7, the first 30 singular values are presented in a logarithmic scale for improved visibility. The close agreement between the singular value spectra across runs within the same pressure conditions demonstrates the reliability of the experimental setup and robust reproducibility of the flow structures captured by the POD method.

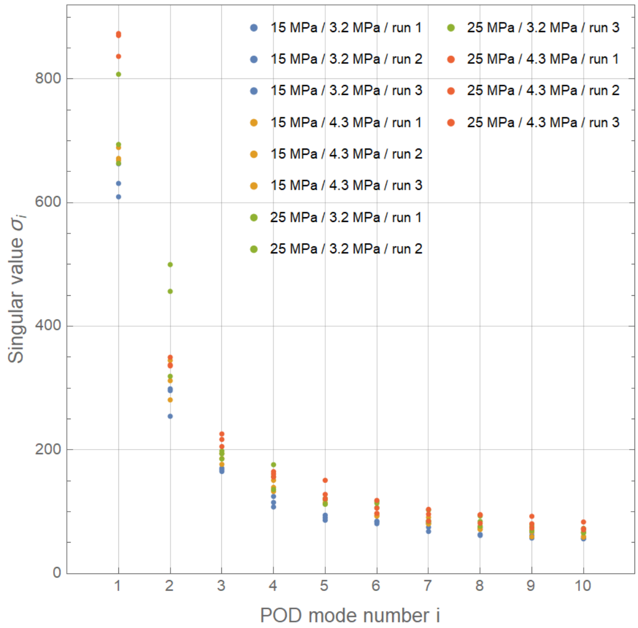


Fig. 6. Singular values, the first 10 modes for each spray run

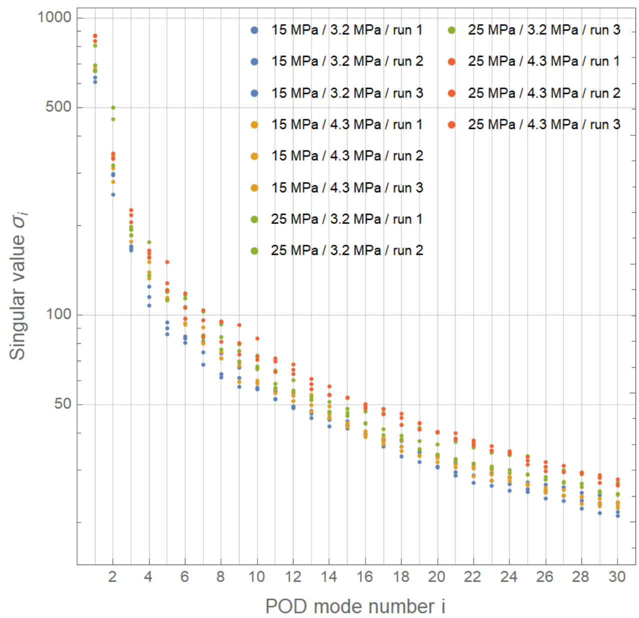


Fig. 7. Singular values, the first 30 modes for each spray run

Each singular value squared $\sigma_i^2$ represents the energy variance captured by the i-th mode. Then, the total energy in POD is defined as the sum of the singular values squared from all modes, i.e.,

$$E_{total} = \sum_{i=1}^{r} \sigma_i^2 \quad (3)$$

As a physical interpretation, the total energy corresponds to the overall variability in the spray over time, i.e., how much the spray pattern changes over time across all snapshots. In general, a higher value of energy corresponds to more dynamics. In Table 2, we show the total energy for all pressure conditions. The close agreement between the energy distributions across runs demonstrates the reliability of the experimental setup and the consistency of the POD decomposition interpretation.

From the moment fuel is injected into the combustion chamber, the jet begins to break up into droplets. The geometric parameters of the injector, such as orifice diameter, length-to-diameter ratio (L/D), and the pressure difference between the injection pressure and chamber pressure, significantly influence the primary breakup. As the fuel jet propagates further into the chamber, it undergoes secondary breakup. This secondary disintegration is driven by aerodynamic drag forces resulting from the chamber's backpressure. Based on Table 2, it was found that increasing the backpressure of gases in the constant volume chamber from 3.2 MPa to 4.3 MPa results in higher energy values, which in turn leads to enhanced spray dynamics caused by more intensive break-up of fuel spray.

Table 2. Total energy from POD decomposition

| Conditions | | Total energy from POD | | |
|---|---|---|---|---|
| Opening pressure [MPa] | Back-pressure [MPa] | run 1 | run 2 | run 3 |
| 15 | 3.2 | 539067 | 604844 | 636939 |
| 15 | 4.3 | 658921 | 735052 | 680911 |
| 25 | 3.2 | 796846 | 899307 | 922222 |
| 25 | 4.3 | 1054458 | 1013955 | 1064898 |

Next, we analyze the relative energy contribution of each mode, defined as:

$$E_i = \frac{\sigma_i^2}{\sum_{j=1}^{r} \sigma_j^2} \tag{4}$$

In Fig. 8, we present the relative energy contribution of each spray injection run on a logarithmic scale. For all experimental runs, the energy contribution of mode 3 is below 10%, mode 8 is below 1%, and mode 30 is below 0.1%.

Further, in Table 3, we present the energy contributions of the first mode (E1), the first two modes (E1–E2), and the first five modes (E1–E5). The first mode captures approximately 70% of the total dynamics in most cases, indicating that the spray is coherent, though not entirely uniform. An exception is observed in two runs conducted under an opening pressure of 15 MPa and a backpressure of 3.2 MPa in the constant volume chamber, where the first mode captures only 55% of the energy. This suggests noticeable secondary dynamics – likely related to the onset of atomization and turbulence. The first two modes account for about 80–83% of the total dynamics, while the first five modes capture approximately 90–92% across all experimental spray runs. These results suggest organized, low-dimensional coherent behaviour, although minor contributions from atomisation or turbulence are still possible.

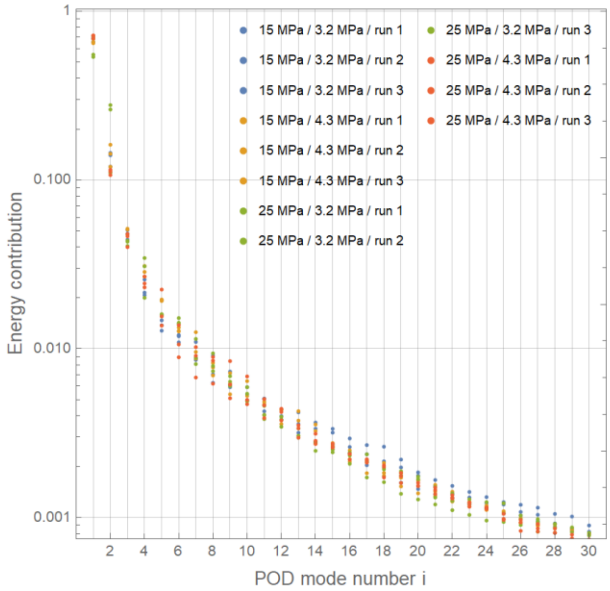


Fig. 8. Energy contribution of the first 30 modes for each spray injection run

Table 3. Energy contribution from the first mode (E1), the first two modes (E1–E2), and the first five modes (E1–E5) for each spray injection run

| Energy contribution | | E1 [%] | | | E1–E2 [%] | | | E1–E5 [%] | | |
|---|---|---|---|---|---|---|---|---|---|---|
| Conditions | | run | | | run | | | run | | |
| Opening pressure [MPa] | Back-pressure [MPa] | 1 | 2 | 3 | 1 | 2 | 3 | 1 | 2 | 3 |
| 15 | 3.2 | 69 | 66 | 69 | 81 | 81 | 83 | 90 | 90 | 91 |
| 15 | 4.3 | 68 | 65 | 66 | 80 | 81 | 80 | 90 | 91 | 90 |
| 25 | 3.2 | 55 | 54 | 71 | 81 | 81 | 82 | 90 | 91 | 90 |
| 25 | 4.3 | 72 | 69 | 72 | 83 | 80 | 83 | 90 | 90 | 92 |

The energy contribution alone is not a sufficient indicator for fully characterizing our experimental setup and spray pressure conditions. Therefore, we proceed with analyzing POD spatial modes and temporal coefficients.

## 4.2. Spatial modes analysis

The spatial modes from the *U* matrix obtained from the POD analysis are a valuable source of information about the spray structure. Shadow images of the spatial modes, calculated for run 1 of each experimental setup, are presented in Fig. 9 and Fig. 10 for opening pressures of 15 MPa and 25 MPa, respectively. Selected modes are shown for backpressures of 3.2 MPa and 4.3 MPa.

In POD analysis, Mode 0 represents the overall geometric shape of the fuel spray, resulting from preprocessing data centering, while Mode 1 corresponds to the dominant structure, such as the cone shape. The number of times a spatial mode changes sign (observed as a black-to-white color transition in Fig. 9 and Fig. 10) can provide information for distinguishing between coherent dynamics and high-frequency structures, such as those associated with atomization.

Lower-order POD spatial modes represent the spray's core and primary breakup structures. The backpressure of gases in the constant-volume chamber directly influences the shape of the diesel fuel spray and its atomization. The intensity at the center of the spatial mode provides insight into the spray's core dynamics. Furthermore, the symmetry of the mode shapes, as seen in Fig. 9 and Fig. 10, indicates that the spray fluctuates in a balanced way on both sides of the spray axis.

Higher-order POD spatial modes can represent droplet behavior, turbulence, and noise. The disintegration of the diesel fuel spray depends on instabilities caused by aerodynamic drag forces. Due to the impact of aerodynamic forces exerted by the gas, the spray surface is subject to violent disturbances, particularly in the outer regions. The edges highlighted in the spatial modes, as seen in Fig. 9 and Fig. 10, suggest that the spray boundary is dynamically active. In these regions, intense secondary breakup occurs, forming cloud-like structures composed of dispersed droplets. Simultaneously, an increase in the cone angle of the fuel spray is observed.

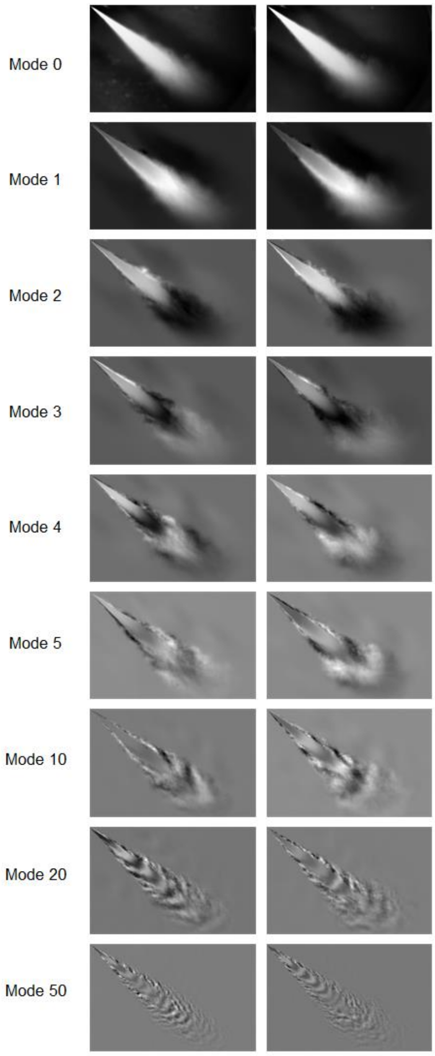


Fig. 9. Spatial mode shapes for opening pressure: 15 MPa with backpressures of 3.2 MPa (left) and 4.3 MPa (right)

Furthermore, if a mode is localized upstream, it may indicate nozzle fluctuations in higher-order modes or injection irregularities in lower-order modes. On the other hand, if the mode is localized downstream, it may point to droplet cloud dispersion or final breakup events.

The interpretation of spatial modes very much depends on the resolution of the snapshots and the physical distance represented by each image pixel. An overall interpretation for mode shapes is given in Table 4.

Table 4. Spatial modes interpretation

| Modes | Interpretation |
|---|---|
| Mode 0 | The mean through all snapshots, i.e., the baseline structure |
| Mode 1 | Represents the dominant structure, like the cone shape |
| Lower Modes | Represent spray core and primary breakups |
| Higher Modes | Represent turbulence, droplet behavior, or noise |

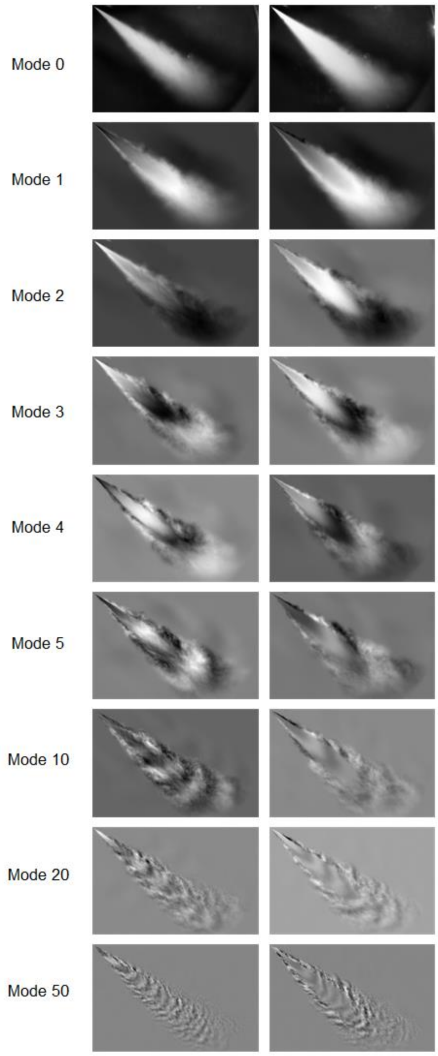


Fig. 10. Spatial mode shapes for opening pressure: 25 MPa with backpressures of 3.2 MPa (left) and 4.3 MPa (right)

## 4.3. Temporal coefficients analysis

For a better understanding of the dynamic behavior of the spray, we also analyze the temporal coefficients obtained from POD. By temporal coefficients analysis, it is possible to determine if the spray shows oscillatory behavior, random fluctuations, or other sudden transient events.

Temporal coefficients, calculated from run 1 of each experimental setup, for selected modes are shown in Fig. 11 and Fig. 12 for opening pressures of 15 MPa and 25 MPa, respectively. These coefficients indicate the contribution of each spatial mode over time and reflect the underlying flow dynamics. Analysis of higher-order modes confirms the presence of complex oscillatory and transient behaviors, which are characteristic of turbulent atomization, droplet interactions, and breakup phenomena.

Additionally, spectral analysis of the temporal signals could be applied to identify dominant frequencies, offering a more quantitative measure of spray behavior.

## 5. Conclusions

In this work, we demonstrated the applicability of the POD method for analyzing the fuel spray atomization process. By decomposing the complex spray dynamics into spatial modes and temporal coefficients, we characterized the dominant structures and their evolution over time.

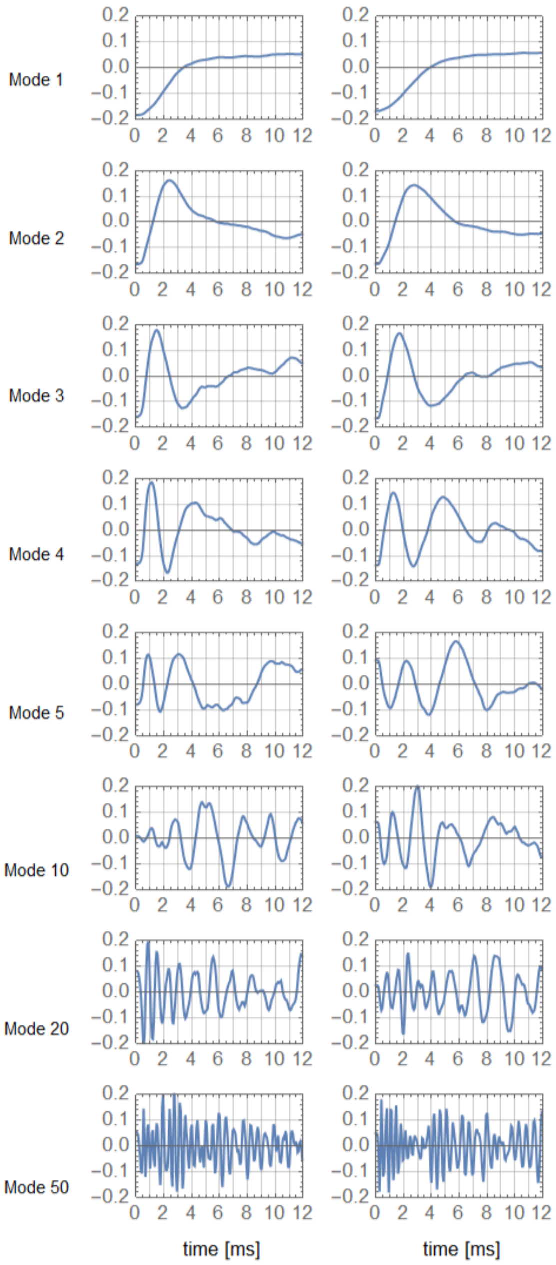


Fig. 11. Temporal POD coefficients for an opening pressure of 15 MPa and backpressures of 3.2 MPa (left) and 4.3 MPa (right)

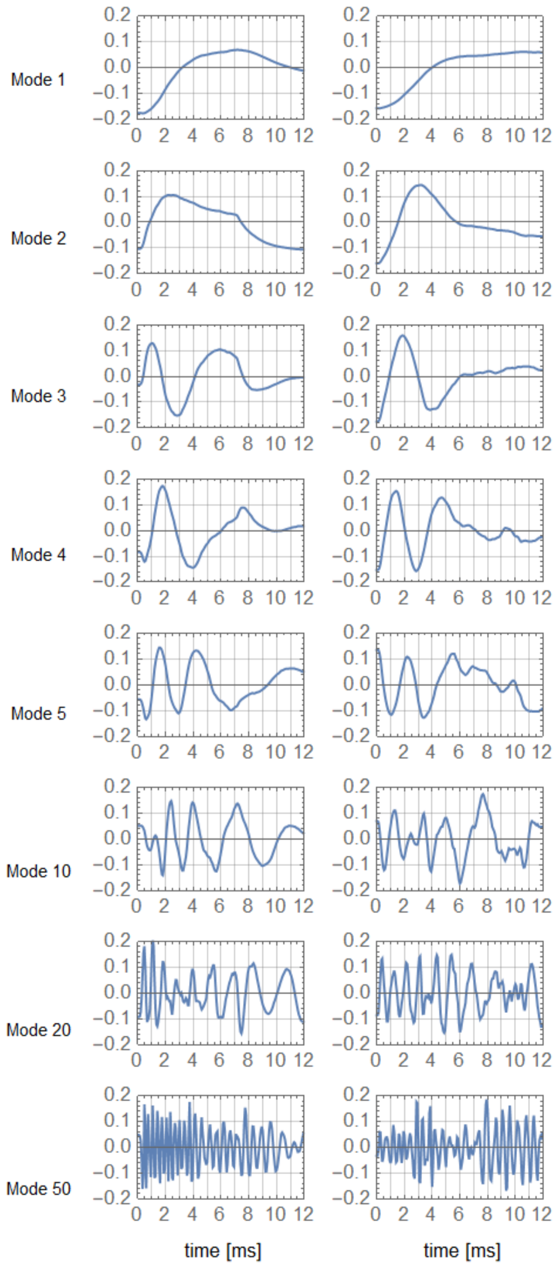


Fig. 12. Temporal POD coefficients for an opening pressure of 25 MPa and backpressures of 3.2 MPa (left) and 4.3 MPa (right)

The consistency of the POD results across repeated tests under the same operating conditions confirms the reliability of the experimental setup and POD methodology. The analysis of singular values showed that the fuel spray is largely governed by a few dominant modes, with the first mode capturing approximately 70% of the total energy under most experimental conditions. Increased backpressure in the constant volume chamber was shown to enhance spray dynamics by increasing the energy associated with secondary breakup and turbulent dispersion. The POD spatial modes provided valuable information about the effects of nozzle fluctuations, core dynamics, and droplet dispersion at different stages of spray development. The temporal coefficient analysis confirmed the presence of oscillatory and transient behaviors, representing complex atomization processes. It should be emphasized that the test results and their analysis are valid only for the specific fuel injection parameters presented in this work and for the Mie scattering measurement method. The POD method can be used to analyze droplets in a fuel spray in terms of the general structures (modes) present. Therefore, information about which structures dominate the fuel atomization and air mixing process, depending on the injection parameters, can be utilized in the design phase of marine fuel injection systems.

This work's findings suggest that POD can be a powerful tool for optimizing the fuel atomization process in marine diesel engine injectors, supporting future efforts to design more efficient and cleaner combustion systems. It should be noted, however, that the possibility of analyzing the results of fuel spray and spray dynamics tests using POD depends on the specific optical measurement method employed.

**Acknowledgments**

The authors gratefully acknowledge Prof. Jerzy Kowalski for his support and collaboration, and Dr. Piotr Jaworski for his technical assistance during the experimental investigations.

## Nomenclature

| | |
|---|---|
| CI | compression ignition |
| CNG | compressed natural gas |
| DI | direct injection |
| LPG | liquified petroleum gas |
| POD | proper orthogonal decomposition |
| SI | spark ignition |
| SVD | singular value decomposition |
| U | spatial mode matrix |
| $\sigma_i$ | singular value for i-th mode |
| $\Sigma$ | singular values matrix |
| V | temporal coefficient matrix |

## Bibliography

[1] Berkooz G, Holmes P, Lumley JL. The proper orthogonal decomposition in the analysis of turbulent flows. Annu Rev Fluid Mech. 1993;25(1):539-575. https://doi.org/10.1146/annurev.fl.25.010193.002543

[2] Chen H, Hung DL, Xu M, Zhuang H, Yang J. Proper orthogonal decomposition analysis of fuel spray structure variation in a spark-ignition direct-injection optical engine. Exp Fluids. 2014;55:1-12. https://doi.org/10.1007/s00348-014-1703-y

[3] Deng J, Wang X, Wei Z, Wang L, Wang C, Chen Z. A review of NOx and SOx emission reduction technologies for marine diesel engines and the potential evaluation of liquefied natural gas fuelled vessels. Sci Total Environ. 2021;766:144319. https://doi.org/10.1016/j.scitotenv.2020.144319

[4] Du W, Zhang Q, Zhang Z, Lou J, Bao W. Effects of injection pressure on ignition and combustion characteristics of impinging diesel spray. Appl Energy. 2018;226:1163-1168. https://doi.org/10.1016/j.apenergy.2018.06.032

[5] Ganti H, Khare P. Data-driven surrogate modeling of multiphase flows using machine learning techniques. Comput Fluids. 2020;211:104626. https://doi.org/10.1016/j.compfluid.2020.104626

[6] Grochowalska J. Analysis of the macrostructure of the fuel spray atomized with marine engine injector. Combustion Engines. 2019;179(4):80-85. https://doi.org/10.19206/CE-2019-413

[7] Grochowalska J, Jaworski P, Kapusta Ł. Analysis of the structure of the atomized fuel spray with marine diesel engine injector in the early stage of injection. Combustion Engines. 2023;195:97-103. https://doi.org/10.19206/CE-168394

[8] Hu N, Zhou P, Yang J. Reducing emissions by optimising the fuel injector match with the combustion chamber geometry for a marine medium-speed diesel engine. Transp Res D Transp Environ. 2017;53:1-16. https://doi.org/10.1016/j.trd.2017.03.024

[9] International Maritime Organization. Fourth Greenhouse Gas Study 2020. London: IMO 2020 (accessed on 2025.05.06) https://www.imo.org/en/ourwork/Environment/Pages/Fourth-IMO-Greenhouse-Gas-Study-2020.aspx

[10] Kafar L, Merkisz J, Piaseczny L. Fuel spray model in a medium speed marine engine – a simulation. Combustion Engines. 2006;126(3):63-76. https://doi.org/10.19206/CE-117345

[11] Kapitza L, Imberdis O, Bensler HP, Willand J, Thévenin D. An experimental analysis of the turbulent structures generated by the intake port of a DISI-engine. Exp Fluids. 2010;48:265-280. https://doi.org/10.1007/s00348-009-0736-0

[12] Kistler. Piezoresistive high pressure sensor. 2014 (accessed on 2025 May 6). https://www.kistler.com/type=669&fid=61054&model=document&callee=frontend

[13] Lewińska J, Kapusta ŁJ. Analysis of the microstructure of the fuel spray atomized by marine injector. Combustion Engines. 2017;169(2):120-124. https://doi.org/10.19206/CE-2017-221

[14] Lumley JL. Computational modeling of turbulent flows. Adv Appl Mech. 1979;18:123-176. https://doi.org/10.1016/S0065-2156(08)70266-7

[15] Ma H, Wu X, Feng F, Wang D, Yang C, Zhuo C. An experimental study on fuel spray-induced vortex-like structures. Exp Therm Fluid Sci. 2014;57:335-343. https://doi.org/10.1016/j.expthermflusci.2014.05.013

[16] Najar I, Buchholz B, Stengel B, Fink C, Hassel E. Influence of the fuel properties on the injection process and spray development in a large ship diesel engine. In: ILASS–Europe 2017, 28th Conf on Liquid Atomization and Spray Systems; 2017 Sep 6-8; Valencia, Spain. https://doi.org/10.4995/ILASS2017.2017.4787

[17] Salvador FJ, Gimeno J, De la Morena J, González-Montero LA. Experimental analysis of the injection pressure effect on the near-field structure of liquid fuel sprays. Fuel. 2021;292:120296. https://doi.org/10.1016/j.fuel.2021.120296

[18] Soid SN, Zainal ZA. Spray and combustion characterization for internal combustion engines using optical measuring techniques – a review. Energy. 2011;36(2):724-741. https://doi.org/10.1016/j.energy.2010.11.022

[19] Viana M, Hammingh P, Colette A, Querol X, Degraeuwe B, de Vlieger I, van Aardenne J. Impact of maritime transport emissions on coastal air quality in Europe. Atmos Environ. 2014;90:96-105. https://doi.org/10.1016/j.atmosenv.2014.03.046

[20] Weiss J. A tutorial on the proper orthogonal decomposition. In: AIAA Scitech 2019 Forum; 2019 Jan 7-11; San Diego, CA. Reston (VA): AIAA; 2019. Paper No.: AIAA 2019-3333. https://doi.org/10.2514/6.2019-3333

[21] Wrzask K, Kowalski J, Le VV, Nguyen VG, Cao DN. Fault detection in the marine engine using a support vector data description method. J Mar Eng Technol. 2024;23(6):412-422. https://doi.org/10.1080/20464177.2024.2318844

[22] Yao C, Geng P, Yin Z, Hu J, Chen D, Ju Y. Impacts of nozzle geometry on spray combustion of high pressure common rail injectors in a constant volume combustion chamber. Fuel. 2016;179:235-245. https://doi.org/10.1016/j.fuel.2016.03.097

[23] Zhang Z, Zhang P, Chen H, Wu H, Geng L, Zhang W et al. Optical study on the spray and combustion characteristics of diesel-biodiesel-alcohol blend fuels on a constant volume combustion chamber. J Energy Inst. 2024;117:101779. https://doi.org/10.1016/j.joei.2024.101779



Joanna Grochowalska, DEng. – Faculty of Mechanical Engineering and Ship Technology, Gdansk University of Technology, Poland.

e-mail: *joanna.lewinska@pg.edu.pl*



Klaudia Wrzask, DEng. – Faculty of Mechanical Engineering and Ship Technology, Gdansk University of Technology, Poland.

e-mail: *klaudia.wrzask@pg.edu.pl*



Łukasz Jan Kapusta, DEng. – Faculty of Power and Aeronautical Engineering, Warsaw University of Technology, Poland.

e-mail: *lukasz.kapusta@pw.edu.pl*